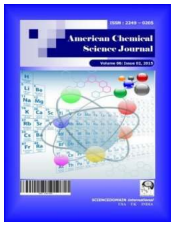

American Chemical Science Journal
12(4): 1-11, 2016, Article no.ACSJ.22771
ISSN: 2249-0205

SCIENCEDOMAIN *international*
www.sciencedomain.org

Brazilian Kaolin Wastes: Synthesis of Zeolite P at Low-Temperature

M. Rodrigues[1*], A. G. Souza[2] and I. M. G. Santos[2]

[1]Flotation Laboratory, Federal Institute of Education, Science and Technology, 58432-300, Campina Grande, Paraíba, Brazil.
[2]Fuels and Materials Laboratory, Department of Chemistry, Federal University of Paraíba, 58059-900, João Pessoa, Paraíba, Brazil.

Authors' contributions

This work was carried out in collaboration between all authors. Author MR designed the study, managed the literature searches, wrote the protocol and wrote the first draft of the manuscript. Authors AGS and IMGS managed and performed the spectroscopic analysis of the study and revised the manuscript. All authors read and approved the final manuscript.

Article Information

DOI: 10.9734/ACSJ/2016/22771
Editor(s):
(1) Francisco Marquez-Linares, Full Professor of Chemistry, Nanomaterials Research Group School of Science and Technology, University of Turabo, USA.
Reviewers:
(1) Marten Ternan, University of Ottawa, Ontario, Canada.
(2) M. C. Somasekhara Reddy, Jawaharlal Nehru Technological University, Hyderabad, India.
Complete Peer review History: http://sciencedomain.org/review-history/12995

Original Research Article

Received 26th October 2015
Accepted 7th January 2016
Published 16th January 2016

ABSTRACT

The synthesis of zeolite in forms suitable for industrial applications is of great importance, mainly as ion exchange material, molecular sieves, adsorbents and catalyst. This paper deals with synthesizing zeolite P using waste kaolinite as starting material (from Brazilian industry ores). The material was characterized by chemical element analysis (FRX), X-ray diffraction (XRD), scanning electron microscopy (SEM), infrared and Raman spectroscopies. With promissory results, although traces of other zeolitic products, such as Zeolite LTA and Zeolite Y, the XRD characteristic peaks attributed to the formed zeolite were confirmed by the 39-0219 (NaP1) cards of JCPDS. The synthesis products are of interest as they can be used in several environmental applications. The photocatalytic activity of prepared material was tested for discoloration process of Remazol Golden Yellow (RNL) dye in aqueous solution under UV irradiation.

Keywords: Low-temperature synthesis; kaolin waste; fluoride media; zeolitic products.

**Corresponding author: E-mail: marceloquimica@gmail.com;*

1. INTRODUCTION

In Brazil, in three regions (south, north and northwest) stands out for having the most important international kaolin deposits for the paper and ceramics industries. During the processing steps for purifying raw kaolin, waste is produced and stored in settling ponds which occupy large area. This situation presents a problem due to the impact on the environment. Kaolin waste is unsuitable for use in paper-making industries; however, this material has the potential of being used in other applications, such as: alumina production, refractories, pozzolans and synthesis of zeolitic materials [1]. Zeolites are microporous high-internal-surface crystalline and hydrated aluminosilicates of alkali and alkaline earth cations with a rigid three-dimensional structure, that framework consists of AlO_4^{5-} and SiO_4^{4-}. Tetrahedral units linked through shared oxygens. Since the pioneering work [2] Synthetic zeolites are usually produced under varying conditions and techniques [3-5]. The general method of zeolite production involves dissolving precursor materials include SiO_2, Al_2O_3 and structure directing agents (SDAs) sources into an alkaline solution. Other variables including the mineralizing agent (such as F^-) and your concentrations have also resulted in new crystalline materials. Most zeolites probably could be obtained at 25 – 250℃ in alkaline solutions. Varying the reaction medium composition and conditions, it's possible to synthesize different zeolites structures or the same product with different chemical compositions. Some conditions of extreme importance in the synthetic zeolites characteristics are the Si/Al ratio: >1, should be the higher reaction temperature (125 – 200℃, under autogenous pressure in autoclaves); <1, synthesis occurs at 25 – 125℃ and zeolites with Si/Al = 1 are obtained at 100 – 150℃. At higher crystallization temperature, there will be a smaller pore volume. The synthesis in the presence of fluoride produces high silica zeolites with a smaller number of defects than in alkaline media and also, one has the possibility of growing single crystals large enough for direct structure. Besides, it allows one to carry out at lower pH than when using OH- [6-15].

Several researchers reported the catalytic role of fluoride species for silicates hydrolysis and condensation [16]. From clay minerals, it is possible to synthesize crystalline aluminosilicate zeolites [17-20]. The literature report that the kaolinite properties are not improved by chemical methods, being a low reactivity material in strongly acidic or alkaline conditions [21-27]. After a calcination (550 – 950℃) yields a more reactive phase (metakaolinite) due to loss of structural water, associated with structure reorganization [28-34].

Zeolite P can be synthesized from various silica-aluminium sources and methods, for examples, using Brazilian kaolin from various sources at 100℃ in 4 days, by the alkaline fusion procedure [35]; from coal fly ash by agitation at 120℃ [36] or from sodium aluminate and sodium silicate solution by hydrothermal treatment in microwave oven [37]. The characterisation and crystal chemistry of NaP zeolites has been controversial for many years. Owing to what was referred to by Hansen et al. [38] it has been difficult to distinguish between different NaP phases and to understand their composition and structure. Although all P zeolites are characterised by the same framework topology, which is the GIS net (named after the natural zeolite gismondine), the formula, symmetry and structure of samples of different composition—which means samples of different Si–Al ratio, Na content and hydration level—were found to be difficult to establish. The main reason for this state of affairs is the high flexibility of the Si–Al linkage in a framework, which has been described being 'the most open (tetrahedral) framework type generated so far [38,39]. A phase called Na-P1 was refined in *I*4 [40]. For this phase, a unit cell content of $Na_6Al_6Si_{10}O_{32}{\cdot}12H_2O$ was adopted. Barrer et al. [41] claimed apparently three polymorphs of zeolite Na-P: cubic (Na-P1), tetragonal (Na-P2) and more rarely orthorhombic (Na-P3). Na-P1 has been described as being body-centered tetragonal with a unit cell of pseudo-cubic geometry. Many salient features of zeolites dynamics and structure can be deduced from vibrational spectroscopy data, such as infrared (IR) and Raman spectroscopy, and the two kinds of spectroscopies are often complementary [42,43]. In zeolite science Raman spectroscopy seems rather underdeveloped compared with infrared spectroscopy. Therefore, the main purpose of this study was to synthesize zeolite NaP using kaolin waste from the northwest region as the main source of silicon and aluminium, improving crystallization time for lower values at low temperature. The characterization by XRD, FRX, SEM, TG/DTA, Raman and FTIR supported this work. Other primary objective was to determine the activity catalytic for decolorization and mineralization extents of dye wastes. Reactive

azo dyes are the largest group of organic dyes with –N=N– group as a chromophore in the molecular structure. They represent more than a half of the global dye production especially because of their wide usage in dyeing industries due to the simple dyeing procedure [44,45]. Normally zeolites have applications in many technological fields such as catalysis and wastewater treatment [46]. Zeolites can serve as hosts to activate transition metal ions, offering a unique ligand system with multiple types of coordination for cations. Zeolites are three-dimensional aluminosilicates containing exchangeable cations that act as Lewis acid sites. The framework oxygen atoms of alkali exchanged zeolites bear partial negative charge and behave as Lewis base [47]. Zeolite P which was synthesized in this paper has a Si/Al ratio of 3.5 which is located in the range of 1–5 for zeolite P.

2. EXPERIMENTAL

2.1 Materials

Kaolin waste (silica and alumina sources used in the synthesis of zeolites) was used as the starting material, after steps grinding by mechanical milling, until fine grained (≤ 74 μm), well crystallized. Without contaminants (muscovite and quartz), kaolinite [$Al_2SiO_5(OH)_4$] may be a good alternative to reuse. Thus, economic advantages would be obtained over chemical reagents used in processes to obtain zeolites that are relatively expensive. Metakaolinite ($Al_2Si_2O_7$) was obtained from calcination of kaolinite at 800℃ for 3 h. Other reagents used in the activation of the starting materials were: sodium fluoride, NaF (99%, Synth) and distilled water. RNL dye, $C_{16}H_{18}N_4O_{10}S_3Na_2$, were kindly provided by a textile manufacturer located in Brazil. This chemical structure is shown in Fig. 1.

2.2 Synthesis

The zeolite synthesis at low-temperature used in this work it´s a modified standard procedure established by IZA because involves pre-treatment and mild-temperature thermal treatment under reflux at approximately 100℃. In the first step, 12,7 g of metakaolinite was mixed with a sodium fluoride, prepared by dissolving 10,4 g of NaF powder in 87,7 mL of distilled water. The resulting synthesis slurry was aged at 50℃ by stirring the mixture for 4 h. After this ageing, the slurry then underwent a thermal treatment by heating at a temperature of approximately 100℃ under reflux system for 96 h. The solid product was filtered and washed with deionized water until the rinsing water reached a pH around 9, centrifuged at 3500 rpm and dried at 105℃ for 24 h. The obtained product was referred to as zeolite P.

2.3 Methods and Characterization

The X-ray diffraction patterns of zeolite P was performed using a Shimadzu diffractometer X/XRD-6000 model Lab using cooper radiation (CuKα1 = 1.5406 Å) and 2θ range of 5 – 50°, at 0.1° intervals and a counting speed of 0.02°/s. The *Joint committee on powder diffraction standards – International centre for diffraction* (JCPDS-ICD) was reference library that was supplied with the XRD instrument for identify and comparison with the mineral phases present in the sample.

The major oxides and trace elements in kaolin waste were measured by X-ray fluorescence (XRF) spectroscopy, using a Shimadzu XRF-1800 model, wavelength dispersive spectrometer. To prevent interaction of the X-rays with air particles, samples were analysed within a vacuum.

The infrared analyses were carried out in a Varian spectrometer 3100 FT-IR, Excalibur Series model in the 2,000-400 cm^{-1} region (mid-infrared), scan and 4 cm^{-1} resolution, using a diffuse reflectance cell.

The Raman analyses were done in a spectroscopy was measured by a Renishaw inVia Raman Microscope with an argon laser operating at 512 nm as the excitation source.

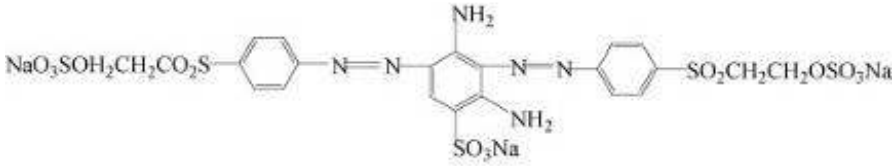

Fig. 1. Chemical structure of Remazol Yellow Gold RNL dye

The synthesized Zeolite P were coated with gold and the morphology was analysed by Scanning Electron Microscopy (SEM) using a Shimadzu SSX-550 Super Scan Scanning Electronic Microscope, with energy dispersive X-ray spectroscopy (EDS) coupled to the SEM was used to identify the chemical composition of a specific area.

The characterization of the precursor (kaolin) was performed by thermogravimetry (TG) and differential thermal analysis (DTA), using a TA Instruments SDT 2960 thermal analyzer. Samples of about 10 mg were heated at 10℃ min^{-1} up to 1000℃, in an air atmosphere, inside alumina pans, with a flow rate of 100 mL min^{-1}.

2.4 The Photocatalytic Activity

Photodecolorization experiments were performed with a photocatalytic reactor system (Fig. 2). During the photocatalytic tests, 100.0 mg of the zeolite P powders was added to a Petri dish containing 15.0 mL of a 10 ppm aqueous solution of RNL with stirring at 5000 rpm/10 min. All of the analyses were performed in triplicate at pH = 6.0. Experiments were conducted in a 10 x 10 x 100 cm^3 lab-made reactor for 5 h using a UVC lamp (λ = 254 nm ≈ 4,9 eV), SuperNiko, model ZG-30T8.

Evaluation of the adsorption and of the photocatalysis was performed by measurement of the discoloration percentage. The decolorization of Remazol dye was analysed by UV–vis spectrophotometer (UV-2550 Shimadzu). The analysis of the resulting solution was performed after centrifugation and filtering of the suspension. The discoloration percentage was obtained from the band at 410 nm, which is assigned to the =N=N- bond, i.e., the azo bond. The values were calculated using a calibration (based on Beer's law were established with the absorbance and the concentration of dye) curve obtained from the intensity of the absorption band at 410 nm of solutions with known concentrations of RNL. Discoloration due to photolysis was subtracted from the discoloration percentage [48].

3. RESULTS AND DISCUSSION

The thermal decomposition of kaolinite is illustrated in the Fig. 3. Both TGA and DTA traces indicate a three stage desorption process. At < 150℃, low temperature release of absorbed water in pores, on the surfaces, (water desorption), which depends on the nature of the kaolinite and the degree of disorder of stacking, and the corresponding weight loss amounts were about 13%. At 150 – 450℃, a weight loss that can be correlated with a pre-dehydration process takes place as a result of the reorganization in the octahedral layer, first occurring at the OH of the surface. After dehydration, kaolinite goes through a pre-dehydroxylation state, at 450-650ºC [49]. According this literature, between ~400–650℃, the kaolinite dehydroxylation occurs, with the transformation to a non-crystalline phase, metakaolinite.

The elemental analysis of sample was conducted by X-ray fluorescence spectrometer (XRF). This analysis was chosen instead of other techniques due to its simpler sample preparation, ability to determine some non-metals and improved precision. The chemical composition of the kaolin waste was determined by means of element chemical analysis by using the X Ray Fluorescence (XRF) technique, and it is shown in Table 1. As can be seen from Table 1, the kaolin sample with SiO_2, Al_2O_3 and K_2O, as the major constituents and content of Fe_2O_3 less than 1%.

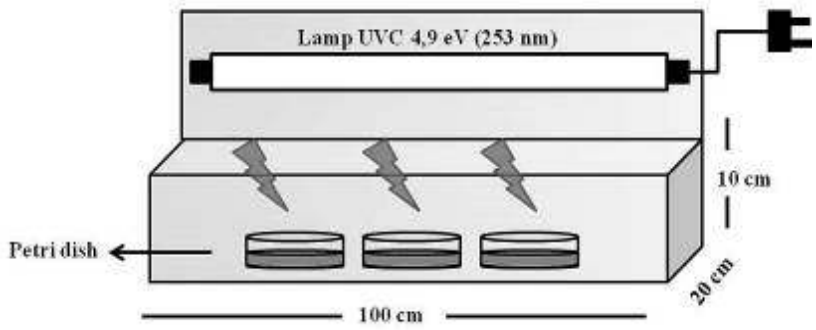

Fig. 2. Apparatus used in the photocatalytic test

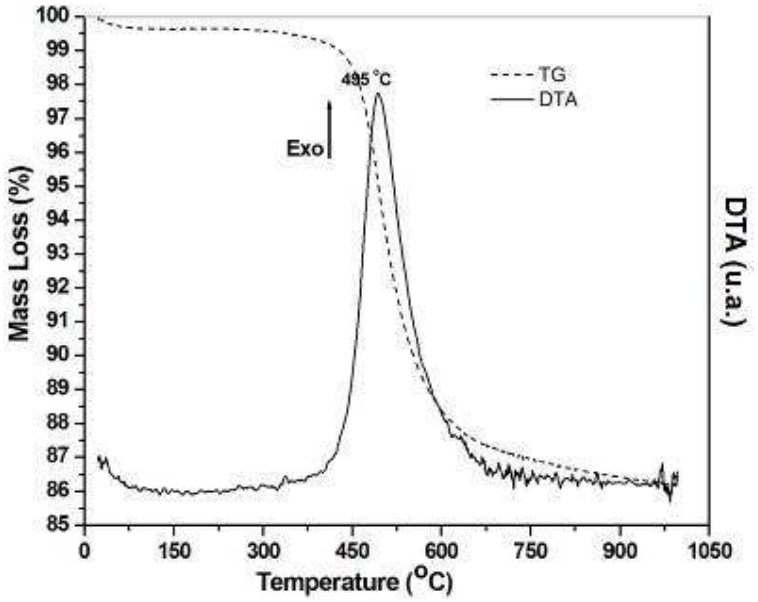

Fig. 3. TG/DTG curves between 10-1000℃ for kaolini te

The amount of SiO_2 and Al_2O_3 within zeolite was lower when compared to waste kaolin. This is may be due to ions dissolution to form a aluminum-silicate gel, which are pre-crystal of zeolite materials, covering the kaolin surface and thus inhibiting the supply of such ions by waste, due to the coverage of these particles surface. Consequently, an increase in Na_2O contents of the products is caused by captured sodium ions, to neutralize the minus charge on aluminate in zeolite structure when crystal is formed [50]. The alkaline solution containing F^- dissolved and reduced the concentration of various impurities, such as Mg, Fe, Ca and K. Zeolites contain natural molecular water as an intracrystalline fluid, which can be removed by elevated temperature and evacuation. The water can normally be re-adsorbed by exposing the crystal to water vapour. The water content of sample which corresponded to the loss of ignition. In this case, extra amount of sodium content which was introduced into the zeolite by exhaustively exchange enhanced the water re-adsorption. The observation concluded that the water content partially attributed to the cation types and their amount present in the zeolite.

In this study, the SiO_2/Al_2O_3 ratio is equal to 3.5 mol, the X-ray diffraction analysis shows the presence of zeolite NaP in the synthesized sample as evidenced from reflections of low intensity near 2θ = 12.4, 17.8, 21.7, 28.2, 33.3, 35.76, 38.01, 42.20 and 44.18. This result indicated that the solid residue from kaolin processing was successfully converted into zeolite-P structure with no amorphous materials. While the peaks positioned in 34.77, 42.19, 42.85 may be zeolite A (LTA) or 34.69, 42.14 and 42.66 zeolite Y (Fig. 4).

Table 1. Chemical composition of the starting material (waste kaolin) and Zeolite P

Constituents	Kaolin	Zeolite-P
	Weight determined (%)	
SiO_2	66.93	38.5
Al_2O_3	24.2	18.7
K_2O	6.91	1.5
Fe_2O_3	0.46	0.6
Na_2O	0.39	11.9
MgO	0.34	0.2
MnO	0.22	0.1
P_2O_5	0.14	tr
CaO	0.08	0.6
TiO_2	0.07	0.2
SO_3	0.03	0.2
ZnO	0.017	0.0104
NbO	0.011	0.0085
ZrO_2	0.043	0.0084
Cl	0.064	0.444
SrO	0.0035	tr

The morphology, size and shape of crystals in the zeolitic material synthesised was observed by Scanning Electron Microscopy (SEM). The zeolite NaP1 (Fig. 5) showed aggregates with no

specific shapes (spherical particles appearance). Particle sizes of about 5 μm of diameter were obtained with a wide particle size distribution - the diameter of the smallest particle could be less than 2 μm. The chemical composition by EDS analysis indicates magnesium presence. Due to its high concentration in the starting material (kaolin waste), this ion was incorporated in the zeolite crystal lattice framework, although the product was rich in aluminum, silicon, oxygen and sodium, characteristic of a typical zeolite.

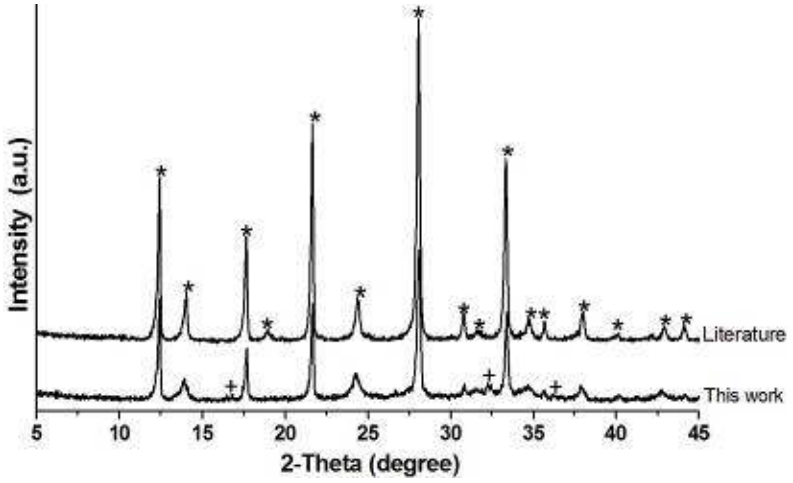

Fig. 4. XRD pattern Zeolite-P synthesised at 100℃. + other s zeolitics phases

Table 2. Result of qualitative analysis of Zeolite P

Phase name	Formula	Space group	DB card number
Zeolite P1, syn	$Na_6Al_6Si_{10}O_{32}$ $(H_2O)_{12}$	82 : I-4	01-071-0962
Zeolite LTA	$Na_{12}Al_{12}Si_{12}O_{48}$ $(H_2O)_{27}$	226 : Fm-3c	01-073-2340
Zeolite Y, syn	$Na_{6.28}D_{44.23}$ $(Al_{56}Si_{136}O_{384})$	227 : Fd-3m,choice-2	01-079-1419

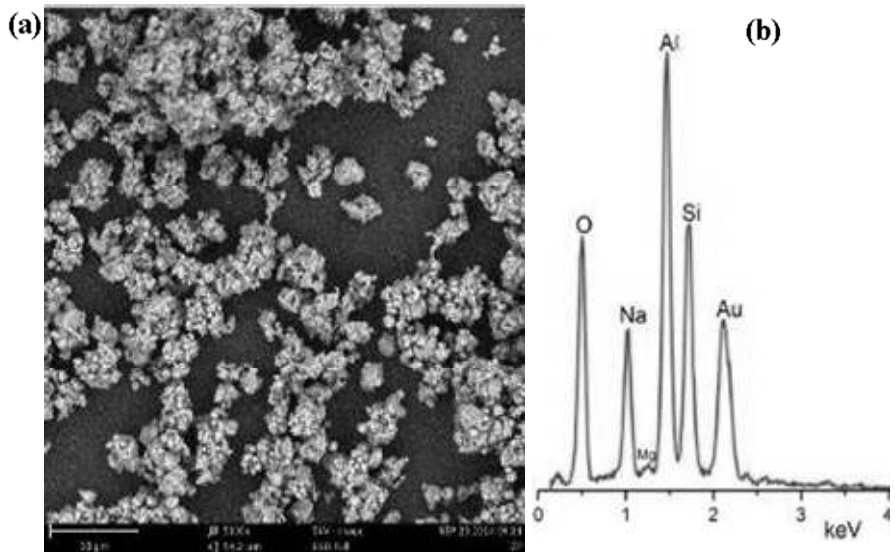

Fig. 5. Zeolite-P synthesised at 100℃. (a) Scanning electr on micrograph (b) EDS spectra

Fig. 6 illustrates the Raman spectrum of Zeolite P with an Si/Al ratio of 3.5. The bands appear at 280, 328, 398, 480 and 508 cm^{-1} [51]. There is a correlation between the ring sizes and the Raman spectra of crystalline zeolites. Structures that are built-up of four-membered rings as the smallest buildin block exhibit the Raman band around 480-520 cm^{-1}. One of these is zeolite NaP (gismondine) built-up of four-membered rings as the smallest building unit. The strongest band at 508 cm^{-1} is assigned to the bending mode of the characteristics 4-membered rings. Zeolites containing exclusively even numbered rings (4MR, 6MR, 8MR, 10MR or 12MR) have Raman frequencies of 390 and 460cm^{-1} and the other band around 500 cm^{-1}. Therefore, the basic assignment of the bands in Raman Spectra for zeolite P should be similar to the one for zeolites A, X and Y. The band at 480 cm^{-1} is assigned to the bending mode of 4-membered Si–O–Al rings. All these results can be influenced and attributed to the difference in the Si/Al when compared with other zeolites with similar symmetries [52].

Infrared spectroscopy (Fig. 7) is another sensitive tool to explore the local chemical environment of atoms. NaP zeolite shown the bending vibration of TO_4 (T = Si, Al) was recorded at around 430–580 cm^{-1}, this bands are related to the deformation mode of the same bonds. The symmetric stretching vibrations of zeolite NaP framework structure of Si–O and Al–O were noticed at, 669 and 710 cm^{-1} [53]. A medium shoulder at 868 cm^{-1} for zeolite NaP1. In addition, one T-O symmetrical stretching for external linkage as indicated by 740 cm^{-1} [54]. According to Huo et al. [55], frequencies near 1000 cm^{-1} are ascribed to asymmetric stretching of bonds Si–O or Al–O. These bands are close to 1000 cm^{-1} in the, which in turn is a feature Si-O-Al bond of the tetrahedron TO_4 and confirm the presence of zeolitic material [56]. The bands with a maximum at 1646 cm^{-1} are peculiar of vibrations of functional groups of OH type and are ascribed to water with zeolitic nature. Similar behavior was found by Albert et al. [57]. Flanigen et al. [7] preview this bands for zeolite P:

UV-vis spectra of the RNL solutions after photocatalytic test under irradiation in time interval of 15 min are presented in Fig. 8. The decrease of absorption spectra and therefore absorbance of samples is indicated by decolorization of the dye, in applied conditions, due to the decrease in the concentration of dye. Since there are partial peaks appearing in the UV–vis spectra the dye isn't completely degraded, but, there was a softening of the bands located at 238 and 292 nm (3-amine-acetanilide group) [58]. Confirmation of the structure undergoes this process can be confirmed through the IR or chromatographic analysis dye. Azo and chromophore group's band (411 nm) has intensity decreased, demonstrating that the zeolite P in study presents some activity to the photodegradation process. This adsorption does not lead to the breaking of the -N=N- bond, and discoloration is simply related to the decrease in the concentration of the RNL adsorbed onto the catalyst after its removal from the solution [48]. A comparison of discoloration due to adsorption and discoloration due to photocatalysis reveals that the percentage increased 17.2%.

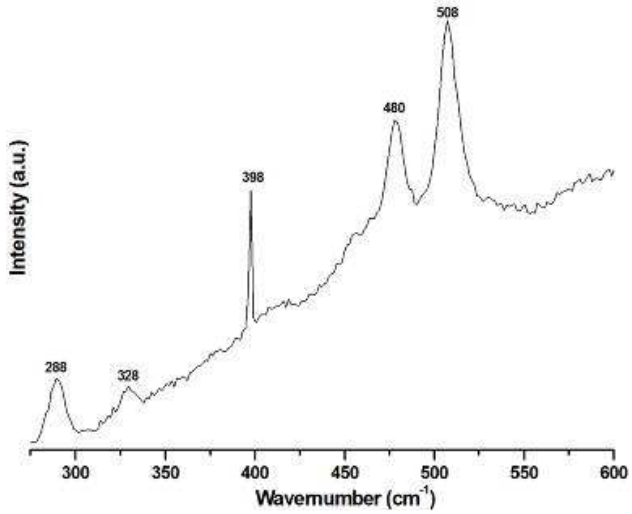

Fig. 6. Raman spectra of Zeolite-P synthesised at 100℃

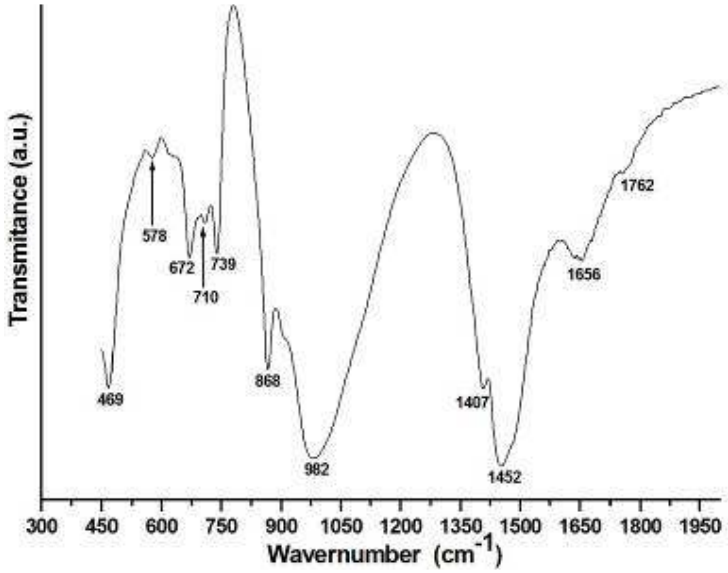

Fig. 7. FT-IR spectra of Zeolite-P synthesised at 100℃

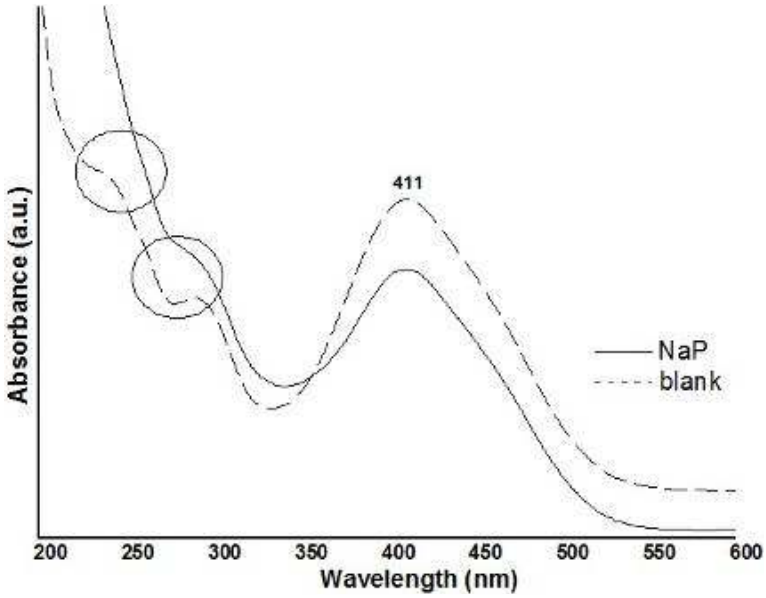

Fig. 8. UV–visible absorption spectra of the textile dye, RNL, after photocatalysis in the presence of NaP irradiated with UV light, comparing to that of the blank

4. CONCLUSIONS

In summary, kaolin wastes from Seridó of Brazilian northwest region refined by mechanical milling and thermally activated is a promising source of silicon and aluminum for the synthesis of zeolite NaP. Mineralogical analysis of the final zeolitic product not showed the presence of others feedstock phases of solid residue, which indicated complete change. The synthesised zeolite NaP was tested for photocatalytic degradation of Remazol Yellow Gold (commercial azo dye). This work demonstrates this materials showing significant potential for using as a photocatalytic material for effluent treatment.

COMPETING INTERESTS

Authors have declared that no competing interests exist.

REFERENCES

1. Dutta PK, Shieh DC, Puri M. Correlation of framework Raman bands of zeolites with structure. Zeolites. 1988;8:306-309.
2. Barrer RM, Cole JF, Sticher H. Chemistry of soil minerals. Part V. Low temperature hydrotermal transformations of kaolinite. Journal of the Chemical Society A: Inorganic, Physical, Theoretical. 1968; 2475-2485.
3. Barrer RM. Hydrothermal chemistry of zeolites, 1st ed., London: Academic Press, 1982.
4. Jacobs PA, Martens JA. Synthesis of high-silica aluminosilicate zeolites, 1st Ed., New York: Elsevier Science; 1987.
5. Szoztak R. Handbook of Molecular Sieves, 1st ed., London: Blackie Academic and Professional; 1998.
6. Corma A. Towards a rationalization of zeolite and zeolitic materials synthesis. Studies in Surface Science and Catalysis. 2004;154:25-40.
7. Flanigen EM. Advances in Chemistry. 2nd ed., Washington: American Chemical Society, A review and new perspectives in zeolite crystallization. 1973;121:119-139.
8. Tavolaro A, Mostowicz R, Creaa F, Nastro A, Aielloa R, Nagy JB. Formation of MFI crystalline zeosilites from fluoride-containing silicate gels. Zeolites. 1992; 12(6):756-761.
9. Rees LVC, Chandrasekhar S. Hydrothermal reaction of kaolinite in presence of fluoride ions at pH less than 10. Zeolites. 1993;13(1):534-541.
10. Férona B, Guth JL, Mimouni-Erddalanea N. Influence of the presence of NaF on the crystallization of zeolite A (LTA): First evidence for the existence of fluorosodalite, the missing end-member of the halosodalite series. Zeolites. 1994; 14(3):177-181.
11. Koller H, Wolker A, Villaescusa LA, Díaz-Cabañas MJ, Valencia S, Camblor MA. Five-Coordinate silicon in high-silica zeolites. Journal of the American Chemical Society. 1999;121(14):3368-3376.
12. Barrett PA, Camblor MA, Corma A, Jones RH, Villaescusa LA. Synthesis and structure of As-prepared ITQ-4, a large pore pure silica zeolite: The role and location of fluoride anions and organic cations. The Journal of Physical Chemistry B. 1998;102(21):4147-4155.
13. Serrano DP, Van Grieken R, Sanchez P, Sanz R, Rodriguez L. Crystallization mechanism of all-silica zeolite beta in fluoride medium. Microporous and Mesoporous Materials. 2001;46(1):35-46.
14. Kato M, Itabashi K, Matsumoto A, Tsutsumi K. Characteristics of MOR-framework zeolites synthesized in fluoride-containing media and related ordered distribution of Al atoms in the framework. The Journal of Physical Chemistry B. 2003;107(8):1788–1797.
15. Kim DS, Chang J-S, Hwang J-S, Park S-E, Kim JM. Synthesis of zeolite beta in fluoride media under microwave irradiation. Microporous and Mesoporous Materials. 2004;68(1-3):77–82.
16. Schmidt-Winkel P, Yang P, Margolese DI, Chmelka BF, Stucky GD. Fluoride-induced hierarchical ordering of mesoporous silica in aqueous acid-syntheses. Advanced Materials. 1999;11(4):303-307.
17. Boukadir D, Bettahar N, Derriche Z. Synthesis of zeolites 4A and HS from natural materials. Annales de Chimie Science des Matériaux. 2002;27(4):1-13.
18. Klimkiewicz R, Drag EB. Catalytic activity of carbonaceous deposits in zeolite from halloysite in alcohol conversions. Journal of Physics and Chemistry of Solids. 2004;65(2-3):459–464.
19. Baccouche A, Srasra E, Maaoui ME. Preparation of Na-P1 and sodalite octahydrate zeolites from interstratified illite–smectite. Applied Clay Science. 1998;13(4):255-273.
20. Cañizares P, Durán A, Dorado F, Carmona M. The role of sodium montmorillonite on bounded zeolite-type catalysts. Applied Clay Science. 2000;16(5-6):273–287.
21. Lussier R. A novel clay-based catalytic material-preparation and properties. Journal of Catalysis. 1991;129(1):225-237.
22. Murat M, Amorkrane A, Bastide JP, Montanaro L. Synthesis of zeolites from thermally activated kaolinite. Some observations on nucleation and growth. Clay Minerals. 1992;27(1):119-130.
23. Akolekar D, Chaffee A, Howe RF. The transformation of kaolin to low-silica X zeolite. Zeolites. 1997;19(5):359-365.
24. Perissinotto M, Storaro L, Lenarda M, Ganzerla RJ. Solid acid catalysts from clays: Acid leached metakaolin as isopropanol. Journal of Molecular Catalysis A: Chemical. 1997;121(1):1103-109.

25. Chandrasekhar S, Pramada PN. Investigation on the synthesis of zeolite NaX from Kerala kaolin. Journal of Porous Materials. 1999;6(4):283-297.
26. Demortier A, Gobeltz N, Lelieur JP, Duhayon C. Infrared evidence for the formation of an intermediate compound during the synthesis of zeolite Na–A from metakaolin. International Journal of Inorganic Materials. 1999;1(2):129-134.
27. Xu M, Cheng M, Bao X, Liu X, Tang D. Growth of zeolite KSO1 on calcined kaolin microspheres. Journal of Materials Chemistry. 1999;9(12):2965-2966.
28. Mackenzie RC. Differential thermal analysis, vol. 1, 1st Ed., London: Academic Press; 1970.
29. Chorover J, Choi S, Amistadi MK, Karthikeyan KG, Crosson G, Mueller KT. Linking cesium and strontium uptake to kaolinite weathering in simulated tank waste leachate. Environmental Science Technology. 2003;37(10):2200-2208.
30. Zhao H, Deng Y, Harsh JB, Flury M, Boyle JS. Alteration of kaolinite to cancrinite and sodalite by simulated hanford tank waste and its impact on cesium retention. Clays and Clay Minerals. 2004;52(1):1-13.
31. Lin D-Ch, Xu X-W, Zuo F, Long Y-C. Crystallization of JBW, CAN, SOD and ABW type zeolite from transformation of meta-kaolin. Microporous and Mesoporous Materials. 2004;70(1-3):63-70.
32. Covarrubias C, Garcia R, Arriagada R, Yanez J, Garland T. Cr(III) exchange on zeolites obtained from kaolin and natural mordenite. Microporous and Mesoporous Materials. 2006;88(1-3):220-231.
33. Ríos CA, Wiliams CD, Fullen MA. Nucleation and growth history of zeolite LTA synthesized from kaolinite by two different methods. Applied Clay Science. 2009;42(3-4):446-454.
34. Huang S, Jing S, Wang J, Wang Z, Jin Y. White silica obtained from rice husk in fluidized propellant bed. Powder Technology. 2001;117:232-238.
35. Acorsi MM, Schwanke AJ, Penha FG, Pergher SBC, Petkowicz DI. Transformação de caulim em zeólita tipo P. Cerâmica Industrial. 2009;14:28-33.
36. Murayama N, Yamamoto H, Shibata J. Mechanism of zeolite synthesis from coal fly ash by alkali hydrothermal reaction. Int. J. Miner. Process. 2002;64:1-66.
37. Sathupunya M, Gularib E, Wongkasemjit S. ANA and GIS zeolite synthesis directly from alumatrane and silatrane by sol-gel process and microwave technique. Journal of the European Ceramic Society. 2002;22: 2305–2314.
38. Hansen S, Hakansson U, Landa-Canovas AR, Fälth L. On the crystal chemistry of NaP *zeolites.* Zeolites. 1993;13:276-280.
39. Meier WM, Olsen DH. Atlas of zeolite structure types, 4th ed., Zeolites, Butterworth-Heinemann, London; 1996.
40. Hansen S, Fälth L, Andersson S. Structural relationships in tetrahedral frameworks: Reflections on cristobalite. J. Solid State Chem. 1981;39:137-141.
41. Baerlocher CH, Meier WM. Crystal-structure of synthetic zeolite Na-P1, an isotype of gismondine. Z. Kristallogr. 1972;135:339.
42. Barrer RM, Baynham JW, Bultitude FW, Meier WM. Hydrothermal chemistry of the silicates part VIII: Low temperature crystal growth of aluminosilicates, and of some gallium and germanium analogues. J. Chem. Soc. 1959;195-208.
43. Breck DW. Zeolite molecular sieves: Structure, chemistry and use, 1st Ed., New York: John Wiley; 1974.
44. Zhu C, Wang L, Kong L, Yang X, Wang L, Zheng S, Chen F, MaiZhi F, Zong H. Photocatalytic decolorization of AZO dyes by supported TiO_2/UV in aqueous solution. Chemosphere. 2000;41:303–309.
45. Peternal IT, Koprivanac N, Bozic AML, Kusic HM. Comparative study of UV/TiO_2, UV/ZnO and photo-Fenton processes for the organic reactive dye decolorization in aqueous solution. J. Hazard. Mater. 2007;148:477–484.
46. Anandan S, Yoon M. Photocatalytic activities of the nano-sized TiO_2-supported Y-zeolites, J. Photochem. Photobiol. C: Photochem. Rev. 2003;4:5–18.
47. Othman I, Mohamady R, Ibraheem IA, Mohamed MM. Synthesis and modification of ZSM-5 with manganese and lanthanum and their effects on decolorization of indigo carmine dye. Appl. Catal. A. 2006;299:95–102.
48. Sales HB, Bouquet V, Députier S, Ollivier S, Gouttefangeas F, Guilloux-Viry M, Dorcet V, Weber IT, Souza AG, Santos IMG. $Sr_{1-x}Ba_xSnO_3$ system applied in the photocatalytic discoloration of an azo-dye. Solid State Sciences. 2014;28:67-73.
49. Menezes RR, Almeida RR, Santana LNL, Ferreira HS, Neves GA, Ferreira HC.

Utilização do Resíduo do Beneficiamento do Caulim na Produção de Blocos e Telhas Cerâmicos. Revista Matéria. 2007;12(1):226–236.
50. Hildebrando EA, Andrade CGB, Junior CAFR, Angélica RS, Valenzuela-Diaz FR, Neves RF. Synthesis and characterization of zeolite NaP using kaolin waste as a source of silicon and aluminum. Materials Research. 2014;17(1):174-179.
51. Yu Y, Xiong G, Li C, Xiao F-S. Characterization of aluminosilicate zeolites by UV Raman spectroscopy. Microporous and Mesoporous Materials. 2001;46:23-34.
52. Peter-Paul Knops-Gerrits, Dirk E De Vos, Eddy JP Feijen, Peter A Jacobs. Raman spectroscopy on zeolites. Microporous Materials. 1997;8:3-17.
53. Albert BR, Cheetham AK, Stuart JA and Adams CJ. Investigations on P zeolites: synthesis, characterisation, and structure of highly crystalline low-silica NaP. Microporous and Mesoporous Materials. 1998;21:133-142.
54. Fuentes GG, Ruiz-Salvador AR, Mir M, Picazo O, Quintana G, Delgado M. Thermal and cation influence on ir vibrations of modified natural clinoptilolite. micropor. Mesopor. Mater. 1998;20:269-281.
55. Huo Z, Xu X, Lv Z, Song J, He M, Li Z, et al. Thermal study of NaP zeolite with different morphologies. Journal of Thermal Analysis and Calorimetry. 2012;1-5.
56. Demortier A, Gobeltz N, Lelieur JP, Duhayon C. Int. J. Inorg. Mater. 1999;1: 129-134.
57. Zholobenko VL, Dwyer J, Zhang R, Chapple AP, Rhodes NP, Stuart JA. Structural transitions in zeolite P: An in situ FTIR study. Journal of the Chemical Society, Faraday Transactions. 1998; 94(12):1779-1781.
58. Catanho M, Malpass GRP, Motheo AJ, Avaliação dos tratamentos eletroquímico e fotoeletroquímico na degradação de corantes têxteis, Quim. Nova. 2006;29(5): 983-989.

Peer-review history:
The peer review history for this paper can be accessed here:
http://sciencedomain.org/review-history/12995